International Forum on Aeroelasticity and Structural Dynamics
IFASD 2019
9-13 June 2019, Savannah, Georgia, USA

STRUCTURAL DYNAMICS ASSESSMENT ON A FULL-ELECTRIC AIRCRAFT: GROUND VIBRATION TESTING AND IN-FLIGHT MEASUREMENTS

E. Di Lorenzo[1], U. Musella[1], S. Vettori[1], R. Hallez[1], J. Debille[1], B. Peeters[1], W. Flynn[1], P.Z. Csurcsia[1,2]

[1]Siemens Industry Software
Leuven, Belgium
emilio.dilorenzo@siemens.com

[2]Vrije Universiteit Brussel
Brussels, Belgium

Keywords: Ground Vibration Testing, Flutter, Electric Aircraft, Virtual Driving Point

Abstract: Aircraft electrification is going to radically change the air transportation in the future. Being a new technology, it is very important to assess the vibroacoustic behavior of an electric aircraft in order to provide useful information to the design and manufacturing teams on the end-products acoustic and dynamic performances. In this paper an assessment based on the structural dynamics characteristics has been carried out both on the ground and in-flight on the Magnus eFusion, first all-electric aerobatic training airplane in the world. Both challenges and findings related to lightweight aircrafts Ground Vibration Testing (GVT) and in-flight measurements for flutter analysis are discussed. The GVT, required for flutter prediction analysis and Finite Element model update, is typically scheduled very late in the development process, right before the final painting and the maiden flight, in a short time window with the aircraft ready-to-fly: high quality and representative frequency response functions are compulsory and testing time is a constraint. This paper describes a GVT campaign carried out at the Magnus facilities in Hungary where several innovative processing techniques and control algorithms have been used for obtaining the experimental modal model of the full aircraft. Special focus has been given to novel processing techniques with the additional target to identify potential structural nonlinearities by the mean of tailored excitation signals. The results from the GVT campaign have been then used to prepare the in-flight tests. In-flight vibration measurements have been performed with a reduced number of sensors for various flight conditions in order to assess the risk to enter into aerodynamic flutter. Finally the comparison between GVT mode shapes and in-flight ones has been performed.

1 INTRODUCTION

Electric propulsion for aircraft brings many new possibilities for more efficient, more flexible and greener air transportation. New concepts, such as drones or flying taxies, based on all-electrical or hybrid propulsion are being studied to support urban air mobility in the future [1]. The impact of aircraft electric propulsion on exterior radiated noise and cabin comfort has not been assessed extensively and very few detailed experimental analyses have been performed so far. Earlier work [2] and [3] concentrated on design and performance of propulsion systems but with no focus on the noise impact. Interesting work was recently performed by Rizzi [4],

Figure 1: Magnus Fusion aircraft tested with an all-electric propulsion system.

on the annoyance to noise produced by a distributed electric propulsion system. However, this analysis is based on simulated data only and does not contain experimental comparisons. On the other hand, no studies have been found in the literature where the structural performance both on the ground and in-flight of an all-electric aircraft are analyzed. In this work, the structural dynamics analysis of the all-electric aircraft has been performed based on ground and in-flight measurements. The objective is to present the testing methods available to identify the main resonant modes of the aircraft, to be used for flutter prediction and to verify that the modes can also be correctly identified during flight. The Virtual Driving Point (VDP) technique to improve the modal identification of large and dynamically complex structures such as an aircraft has been developed and validated in this challenging case. Furthermore, a nonlinearity assessment based on the use of multisine signals as inputs to the shakers during the Ground Vibration Testing (GVT) is extensively described in the next sections. This procedure allows to detect nonlinearities with a very good level of accuracy. The first part of the paper will go through the Ground Vibration Testing (GVT) measurements and the post-processing techniques used to obtain the experimental modal model of the aircraft. The in-flight measurements are discussed in the second part of the paper and a final comparison between the ground and in-flight results is shown. Ground Vibration Testing (GVT) is part of the aircraft certification process and its purpose is to estimate the aircraft dynamic characteristics (natural frequencies, mode shapes, structural damping coefficients and generalized mass). These results allow to update the FE (Finite Element) model of the structure that is then used for flutter prediction [5]. These tests are performed right before the maiden flight of the aircraft and usually there is always a reduced time slot assigned to the GVT. For this reason, it becomes very important to reduce the test duration and at the same time to improve the test results. In order to achieve a good compromise between the testing time and the achieved results, advanced techniques and new methods are continuously investigated [6]. The investigated airplane is the Magnus Fusion aircraft. The Magnus Fusion 212 is a multi-purpose 2-seater aircraft, see Figure 1. It has a length of 6.7m, height of 2.4m, and a wingspan of 8.3m including winglet, whereas the wing area is 10.59m^2. The eFusion is the all-electric version of the Fusion aircraft, first all-electric aerobatic training aircraft in the world. It is powered by a 60kW Siemens electric drive system. The aircraft is entirely battery-powered and has an endurance of approximately one hour. The aircraft has an empty weight of 410kg and a maximum take-off weight of 600kg. The stall and maneuvering speeds of the aircraft are 35kn and 104kn, respectively.

2 GROUND VIBRATION TESTING (GVT)

In the past years, the so-called Normal Mode Testing has been almost exclusively used for GVT on aircraft since this technique is suited for separating very closely spaced mode shapes. Es-

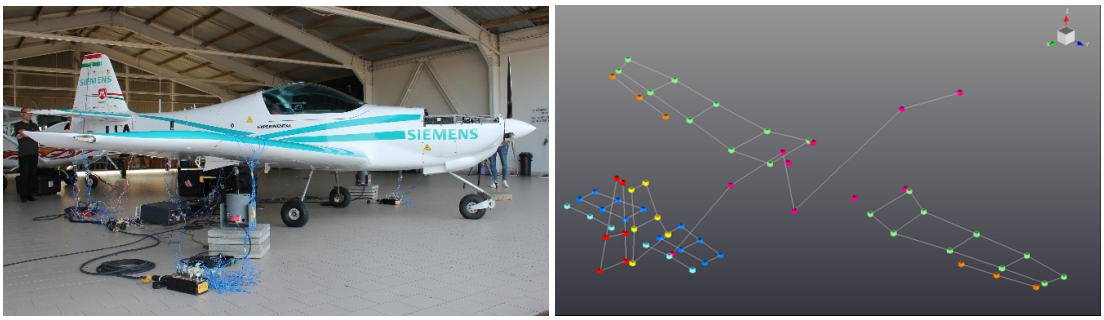

Figure 2: Ground Vibration Testing measurement setup (left) and geometry (right).

sentially it uses an excitation tuned at single frequency lines in correspondence of the modes of the aircraft. Very accurate results could be achieved, but this procedure is very time consuming. This is one of the reasons behind the development of innovative techniques based on the estimation of the modal parameters from broadband Frequency Response Functions (FRFs). FRFs can be obtained by using a wide range of input signals: burst random, stepped sine, swept sine, etc. Often a swept sine is used as it represents a good compromise between the testing time and the excitation levels needed to excite the modes of the aircraft in a wide frequency range. In this work multisines are also used to avoid any spectrum leakage, to reach full non-parametric characterization of the noise and to be able to detect nonlinearities. Among others, the symmetric and antisymmetric modes of the wings and of the movable surfaces are quite important. They are well excited when providing symmetric and antisymmetric excitations to the structure by means of two shakers placed close to the wing tips. This is especially true for small aircraft, whereas for large aircrafts up to 4 or 8 shakers are used. Symmetric excitation is achieved by applying two sweeps in phase, whereas an antisymmetric excitation is obtained by having a 180°shift between the two input signals. One of the drawbacks of using a sinusoidal sweep method is that different sine sweeps must be performed in series in order to compute the system FRFs. The number of performed sine sweeps must be at least equal to the number of inputs to the system, so at least equal to the number of shakers. The modal identification process, therefore, cannot start until all the needed sweeps are performed since all the data are used together to calculate the FRF matrix [7]. Despite this and although sine sweep methods require a longer time duration than the one needed when applying random excitations, swept sine excitation is preferred to random one because it allows a better excitation of all modes of interest by spanning through a certain frequency band. In this paper the structural dynamics performance of the Magnus eFusion all-electric aircraft was investigated. The GVT campaign was performed at the Magnus facility in Hungary [8]. The airplane's tires were deflated in order to reproduce the ideal free-free boundary conditions and two electrodynamic shakers were used to excite the system. They were placed at intermediate wing points as shown in Figure 2.

The response accelerations were measured by using two Simcenter SCADAS systems in a master-slave configuration. 58 monoaxial accelerometers and 11 triaxial accelerometers were used for a total of 91 measurement channels. The triaxial ones were distributed as follows: left and right wing tips (node close to the leading edge), left and right ailerons tips, front node of the fuselage, left and right tips of the horizontal tail, left and right elevators tips, front nodes on the top of the vertical tail and on the rudder, as shown in Figure 2.

2.1 Virtual Driving Point (VDP) technique

Several estimators could be used to calculate the FRFs. The most commonly used one is the so-called H1-estimator, which assumes that there is no noise on the input and consequently that

all the x measurements (the input) are accurate. All noise (n) is assumed to be on the output y. This estimator tends to give an underestimate of the FRF if there is noise on the input. The input spectral density matrix needs to be inverted to compute the FRFs and, for this reason, it must be non-singular. Therefore it should satisfy the following two conditions:

- The number of performed sine sweeps in series must be at least equal to the number of inputs given to the system (e.g. number of shakers used during the tests);
- The forces belonging to the different performed sweeps must not be correlated (i.e. the phase between the inputs needs to change from a sweep to another).

When two shakers are used, for example, then at least two sweeps for each test must be performed. The applied forces during the different runs are usually chosen to have the same amplitude to control the input forces and avoid damaging the structure, while their relative phase changes from a sweep to another for satisfying the second condition. Figure 3 shows the conventional relative phase scheme adopted for a two points excitation configuration: the first sweep is symmetric because the forces are equal both in amplitude and phase, while the second sweep is antisymmetric because the right wing force, i.e. the reference input, keeps a 0° phase while the left wing force switches its phase to 180°, which means that it has an opposite direction with respect to the reference input. Right and left directions are identified with respect to the pilot point of view.

The Virtual Driving Point (VDP) technique [9] is based on the identification of a virtual force and a virtual response. Both are computed starting from the measured forces and responses of the two actual driving points of the system, i.e. the two physical points where the excitation is applied through the two shakers. Thanks to this procedure, each single sweep can be processed individually and a set of FRFs can be extracted. Therefore, each sweep identifies a specific mode set that, in most of the cases, must be combined with the other in order to obtain the final mode set of the system. The VDP mathematical formulation involves both inputs and outputs frequency spectra, which can be respectively expressed as in equations (1) and (2).

$$\{F(\omega)\} = \begin{Bmatrix} F_1(\omega) \\ F_2(\omega) \end{Bmatrix} = \begin{Bmatrix} |F_1(\omega)|e^{j\varphi_1} \\ |F_2(\omega)|e^{j\varphi_2} \end{Bmatrix} \tag{1}$$

$$\{Y(\omega)\} = \begin{Bmatrix} Y_1(\omega) \\ \vdots \\ Y_{N_o}(\omega) \end{Bmatrix} \tag{2}$$

Figure 3: Conventional technique: two sweeps performed by using two shakers in-phase (left) and out-of-phase (right).

Here Y_1 and Y_2 are assumed to be the accelerations measured in correspondence of the two driving points. F_1 is the reference input and F_2 is the delayed input, where the delay is $\varphi = \varphi_2 - \varphi_1$. First of all the amplitude of the virtual force needs to be calculated, as shown in equation (3).

$$|F_v(\omega)| = \sqrt{|F_1(\omega)|^2 + |F_2(\omega)|^2} \tag{3}$$

The virtual acceleration can be computed as in equation (5) taking into account that equation (4), which is obtained stating the equivalence between the complex power of the virtual input F_v and both the actual inputs F_1 and F_2, can be also written substituting accelerations to velocities in case of harmonic vibrations.

$$|F_v(\omega)|V_v(\omega) = |F_1(\omega)|V_1(\omega) + |F_2(\omega)|V_2(\omega) \tag{4}$$

$$Y_v(\omega) = \frac{|F_1(\omega)|Y_1(\omega) + |F_2(\omega)|Y_2(\omega)}{|F_v(\omega)|} \tag{5}$$

For what concerns the virtual force computation, both in terms of amplitude and phase, it is possible to state that, in case of symmetric excitation, the virtual force weighted by its own amplitude is equal to the sum of the two applied forces, each of them weighted by their respective amplitudes. The resulting formula for the virtual force in case of symmetric excitation is described by equation (6).

$$F_v(\omega) = \frac{|F_1(\omega)|F_1(\omega) + |F_2(\omega)|F_2(\omega)}{|F_v(\omega)|} \tag{6}$$

When the excitation is not symmetric and a generic phase lag φ between the inputs is used, a phase correction, whose mathematical proof is not reported here, must be introduced to bring the delayed input F_2 to have the same phase of the reference one in order to be able to sum them up in the F_v computation. Therefore, equations (7) and (8) are the generic expressions for the virtual force and acceleration that can be applied when any φ between the inputs is used. The phase correction turns into a summation when the excitation is symmetric and a subtraction when it is antisymmetric.

$$F_v(\omega) = \frac{|F_1(\omega)|F_1(\omega) + e^{-j\varphi}|F_2(\omega)|F_2(\omega)}{|F_v(\omega)|} \tag{7}$$

$$Y_v(\omega) = \frac{|F_1(\omega)|Y_1(\omega) + e^{-j\varphi}|F_2(\omega)|Y_2(\omega)}{|F_v(\omega)|} \tag{8}$$

After its computation, the virtual acceleration $Y_v(\omega)$ is appended to the vector of the measured responses $\{Y(\omega)\}$, and a new response vector of N_o+1 elements, expressed in equation (9), is obtained.

$$\{Y(\omega)\}_{new} = \begin{Bmatrix} Y_1(\omega) \\ \vdots \\ Y_{N_o}(\omega) \\ Y_v(\omega) \end{Bmatrix} \tag{9}$$

For the single sweep a new data set can be considered: $F_v(\omega)$ represents the so-called virtual force, while the response vector is $\{Y(\omega)\}_{new}$. From this data set, a column matrix of virtual FRFs can be computed by using equation (10).

$$\{H(\omega)\}_v = \{Y(\omega)\}_{new} \frac{1}{F_v(\omega)} \tag{10}$$

The virtual driving point FRF is the last element of the column matrix $\{H(\omega)\}_v$.

Once the virtual FRFs matrices are computed for each single sweep, the modal analysis step can be performed. From the two FRFs sets, $\{H(\omega)\}_{v_{sym}}$ from the symmetric sweep and $\{H(\omega)\}_{v_{ant}}$ from the antisymmetric sweep, two Polymax stabilization diagrams are defined and two groups of system poles, and therefore two different mode sets, are extracted [10]. The system poles are identified according to their symmetric or antisymmetric nature: symmetric mode shapes of the system are well detected only by the symmetric sweep, while the antisymmetric mode shapes are well identified only by the antisymmetric sweep. In order to reconstruct a single and complete mode set for the system, symmetric and antisymmetric modes, respectively extracted from $\{H(\omega)\}_{v_{sym}}$ and $\{H(\omega)\}_{v_{ant}}$, must be grouped together. Mode shapes that are part of the final mode set are vectors, as the one expressed by equation (11), of N_o+1 components, since in the response vector that has been used to compute the FRFs, the additional component $Y_v(\omega)$ related to the virtual response is also present.

$$\{\Psi\}_r = \begin{Bmatrix} \Psi_{1r} \\ \vdots \\ \Psi_{N_o r} \\ \Psi_{vr} \end{Bmatrix} \tag{11}$$

The Ψ_{vr} component of the mode shapes, i.e. their last element, must be deleted because it represents a non physical Degree-Of-Freedom (DOF) which, depending on the scaling scheme that is used, can also influence the values of the modal displacements related to the other DOFs. After the last element of the mode shapes has been deleted, the resulting mode shapes are scaled again to obtain the proper modal parameters.

2.2 GVT results by using VDP technique

At first burst random tests were carried out at different force levels. In a second stage, logarithmic sine sweeps were used to excite the aircraft. Different sweep rates (0.3, 0.6, 1.2 and 2.4 oct/min), directions (sweep up and sweep down) and several force levels (10N, 15N, 20N) were used. Table 1 shows all performed tests.

Table 1: Test conditions performed during the Ground Vibration Testing campaign

Force(N)	**Sweep rate (oct/min)**			
	slow (0.3)	**medium (0.6)**	**fast (1.2)**	**very fast (2.4)**
3	-	up	-	-
10	-	up/down	up/down	-
15	up	up/down	up/down	up/down
20	-	up	-	-

Several runs were performed in order to understand the different behavior at different force levels, which can be considered as an indicator for non-linear effects. The same is true for sweep-up and sweep-down tests which are commonly used in literature to identify the distorted FRF peaks due to the presence of non-linearity effects. Table 2 shows the list of the identified natural frequencies and damping ratios of the first ten modes up to 40 Hz. The nature of the modes is also indicated: S if it is a symmetric mode shape and A if the mode is antisymmetric. The listed modes have been obtained by performing both the standard Multiple-Input-Multiple-Output (MIMO) method for FRFs estimation (left columns) and by using the VDP technique (right columns). In terms of natural frequency there is not a significant difference (difference always below 1.5%), but the damping ratio is altered in most of the modes in the standard measurements set by the fact that we are combining together the symmetric and the antisymmetric runs. Further studies will be conducted to assess the large discrepancies between the two techniques in terms of damping values. These differences are quite evident in case of antisymmetric modes. The well-known Polymax modal parameters estimator has been used for estimating the modal parameters [10].

Table 2: eFusion aicraft mode sets (S: symmetric; A: antisymmetric)

	STANDARD SET		**VDP RECONSTRUCTED SET**			
MODE TYPE	**Frequency (Hz)**	**Damping (%)**	**Frequency (Hz)**	**Damping (%)**	**Δf (%)**	**Δ Damping (%)**
S	10.74	1.94	10.69	2.05	-0.5	5.7
A	15.43	1.63	15.44	2.28	0.1	39.9
S	16.29	3.52	16.35	3.68	0.4	4.5
A	18.33	2.14	18.16	2.29	-0.9	7.0
A	20.24	2.04	20.25	2.09	0.01	2.5
A	23.68	1.43	23.58	2.17	-0.4	51.7
A	27.41	2.93	27.76	4.07	1.3	38.9
A	30.92	2.82	30.45	2.32	-1.5	-17.7
A	36.04	2.65	35.87	2.52	-0.5	-4.9
S	38.51	0.47	38.46	1.25	-0.1	166.0

The eFusion aircraft is characterized by a strong non-linearity around 20 Hz (approximatively in between 19 and 22 Hz). Indeed it is possible to underline in Figure 4 that the actual driving points FRFs are changing when the force level is changing. The peaks are shifting along the frequency axis. In particular, when the forces level increases, the natural frequency decreases.

On the other hand, figure 5 shows the virtual driving points FRFs obtained by applying the VDP method to the symmetric and the antisymmetric sweeps. Here it is possible to recognize the presence of the non-linearity only in the symmetric VDP FRF, since the one extracted by the

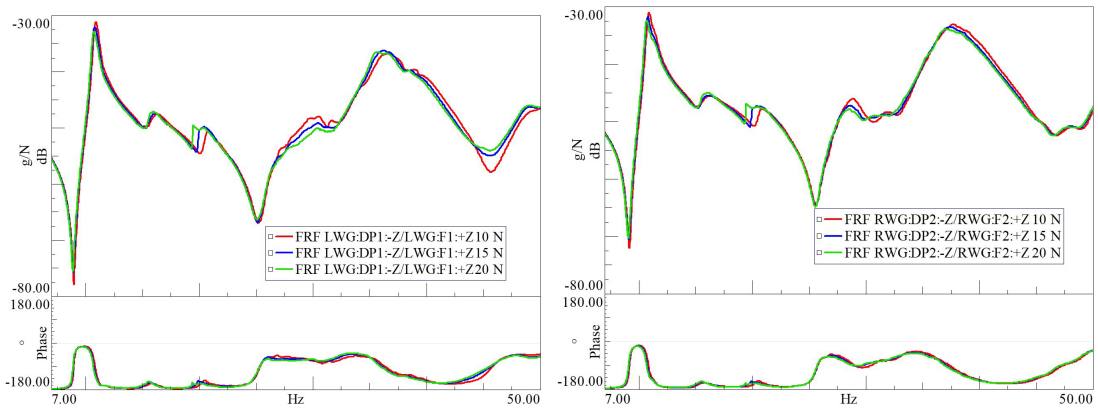

Figure 4: Driving point FRFs for different force excitation levels: 10N, 15N, 20N (left: left wing (LWG); right: right wing (RWG)).

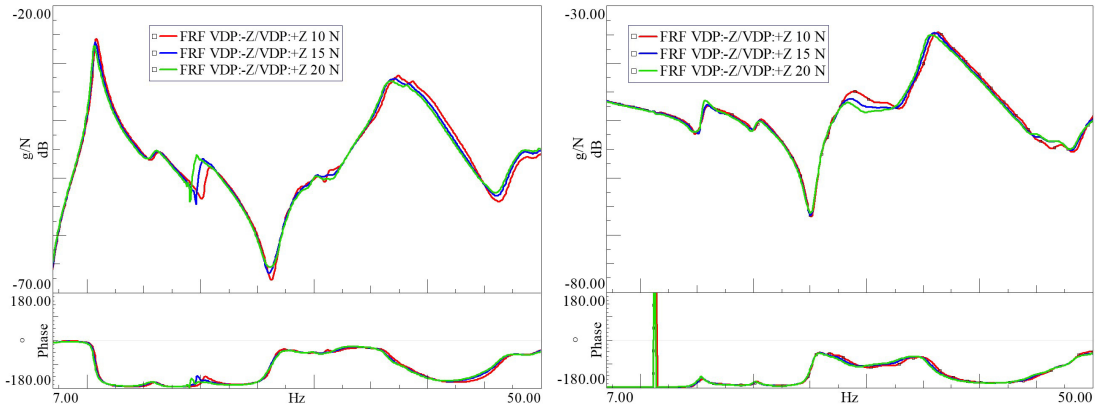

Figure 5: Virtual driving point FRFs (left: symmetric sweep; right: antisymmetric sweep).

antisymmetric sweep does not show any difference around 20 Hz when increasing the forces levels. The mode detected around 20 Hz (mode 5 of both mode sets) has a clear antisymmetric nature, as pointed out in Table 2. It is possible to state that mode 5 of the standard set is influenced by a non-linearity since both sweeps are merged together to obtain the FRFs. On the other hand, mode 5 belonging to the VDP set is not affected by the non-linearity because it is extracted from the antisymmetric sweep only, whose VDP FRF does not show any non-linear effect around 20 Hz. In conclusion, the VDP method allows to isolate the effect of the non-linearities belonging to one run, so that they do not influence the overall results. The root causes of the nonlinearity are not well understood, but it only manifests itself during a symmetric excitation. Figure 6 shows the first four mode shapes of the entire aircraft obtained by using the VDP technique in a frequency range up to 20Hz. A brief description of each mode is also provided in the caption for clarity.

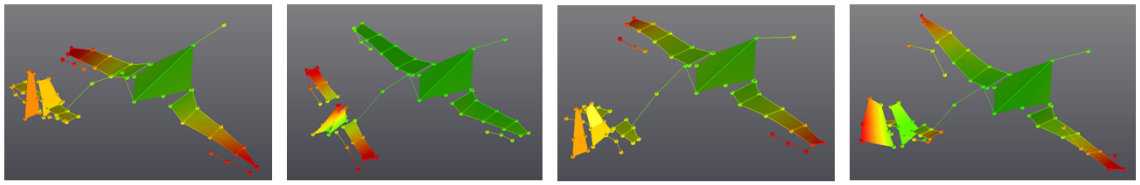

Mode 1, 10.69 Hz, 2.05 %
1st wing bending

Mode 2, 15.44 Hz, 2.28 %
tail torsion

Mode 3, 16.35 Hz 3.68 %
fuselage bending

Mode 4, 18.16 Hz, 2.29 %
1st HTP bending

Figure 6: Aircraft mode shapes obtained by using the VDP technique in a frequency range up to 20Hz.

2.3 Best Linear Approximation approach

The Best Linear Approximation (BLA) has been widely used in the last decades to efficiently estimate FRFs [11], [12], [13]. The BLA of a nonlinear system is an approach of modelling what minimizes the mean square error between the true output of a nonlinear system and the output of the linear model. In this technique, instead of using the classical H1 estimate (cross-power spectral density estimate [11]) and its coherence function, a BLA model is estimated, and the coherence function is split into a) noise level and b) nonlinear contribution estimates. In this work multisine signals are used to avoid any spectrum leakage, to reach full nonparametric characterization of the noise, and to be able to detect nonlinearities. Many users prefer noise excitations, because they are simple to implement, but in this case nonlinearities are not identifiable, and there is a possible leakage error. The best signal that satisfies the desired properties is the user-friendly multisine signal which looks like Gaussian white noise, behaves like it but it is not a noise. It is important to highlight that the multisine excitation is not equivalent to stepped sine excitation [14], [15]. The proposed BLA technique makes use of the knowledge that the excitation signal has both stochastic and deterministic properties. In this work, random phase multisines are used and generated in the frequency domain such that the magnitude characteristic is set by the user, and the phases of the cosines are chosen randomly from a uniformly distribution [16].

2.4 Detection of nonlinearities

This section concerns the analysis of the random phase multisine GVT measurement. The GVT measurement has been executed at three different levels. Figure 7 shows the lowest and highest level excitation signals in the frequency domain. The excitation force is measured with approximately 65 dB SNR. This SNR is sufficiently good to fulfill the assumption on the precise excitation signal measurement. However, it is interesting to point out that the high level excitation signal is 10 dB higher than the low level excitation signal but the SNR improvement is only around 2 dB: the noise level estimate moved together with the excitation signal estimate.

This indicates the presence of (low level) nonlinearities at the excitation system. The analysis of this phenomenon is out of the scope of this paper. Further, in order to simplify the analysis, the output and FRF are shown at the driving points only. In order to ensure that the measured signals are in the steady-state, a simple transient check-up is performed. In this work, each first block (period) is discarded. The sampling frequency is 200 Hz. The period length is 1024 resulting in a frequency resolution of 0.1953 Hz. The smallest excited frequency is 1.1719 Hz, the highest excited frequency is 50.7813 Hz. There are eight different multisine realizations for each input channel per experiment. Each multisine realization is repeated 3 times.

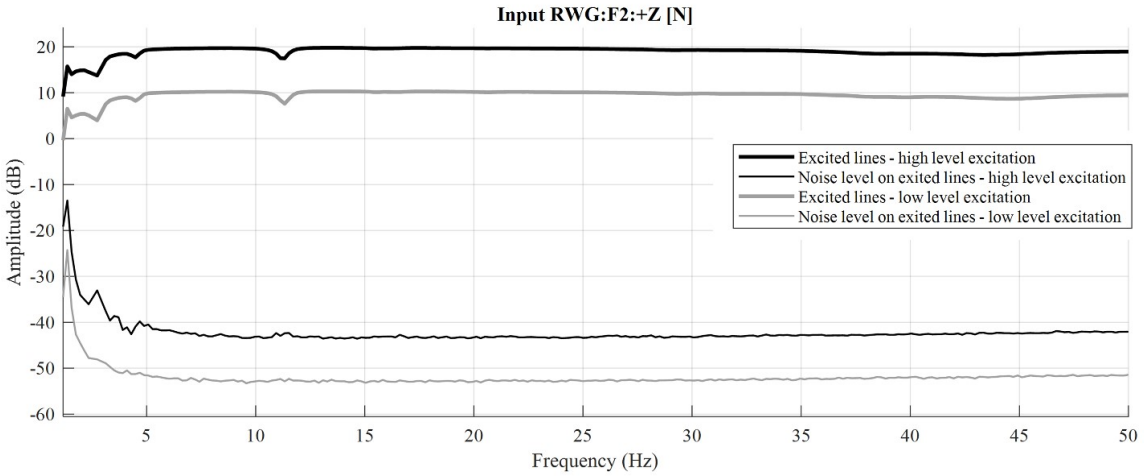

Figure 7: The input (force) signal measured in frequency domain at the low and high amplitude levels.

Figure 4 shows the FRFs at the driving points at different excitation levels. It can be clearly observed that FRFs at different levels differ a lot from each other. This clearly indicated the presence of nonlinearities. The interesting point here is to tell the inexperienced user from only one measurement if the system is linear or nonlinear on that particular level of excitation. The classical H1 framework suggest calculating the coherence function for each frequency line. When the coherence function gives one it means that there is 100% linear correlation between the measured output and input data. When the coherence is lower than one it indicates the presence of (among others) high level noise and/or transient and/or leakage and/or nonlinearities. Since we have used periodic excitation with discarding the delay blocks (transient), we made sure that the lack of coherence stands only for the noise and nonlinearities. In the following part we focus on the left wing FRF high level excitation. In the classical H1 framework the coherence function (pink thick line in Figure 8) is used to estimate the FRF measurements standard deviation (pink thin line in Figure 8). For the numerical computation of coherence function in MIMO case we refer to [17]. Please note that by the use of the proposed BLA framework we can directly estimate the standard deviation and split it into noise level estimation (black thin line in Figure 8) and nonlinearity level estimation (red thin line in Figure 8).

With the help of these curves it is possible to tell how the lack of coherence accounts for the noise and nonlinearity. For instance, the first resonance (around 3 Hz) has an SNR of 35 dB and an SNLR (signal-to-nonlinearity ratio) of 40 dB. This means that at this resonance the main error source is the noise. Looking at the largest resonance (4th resonance at around 12 Hz) one can read that the SNR is around 60 dB and the SNLR is around 30 dB. At this resonance the dominant error source is the nonlinearity. Figure 7 and Figure 8 show the improved FRM, noise and nonlinearity estimates by taking into account all the different realizations and experiments. The question arises: what would be the noise and nonlinearity level on an arbitrary chosen

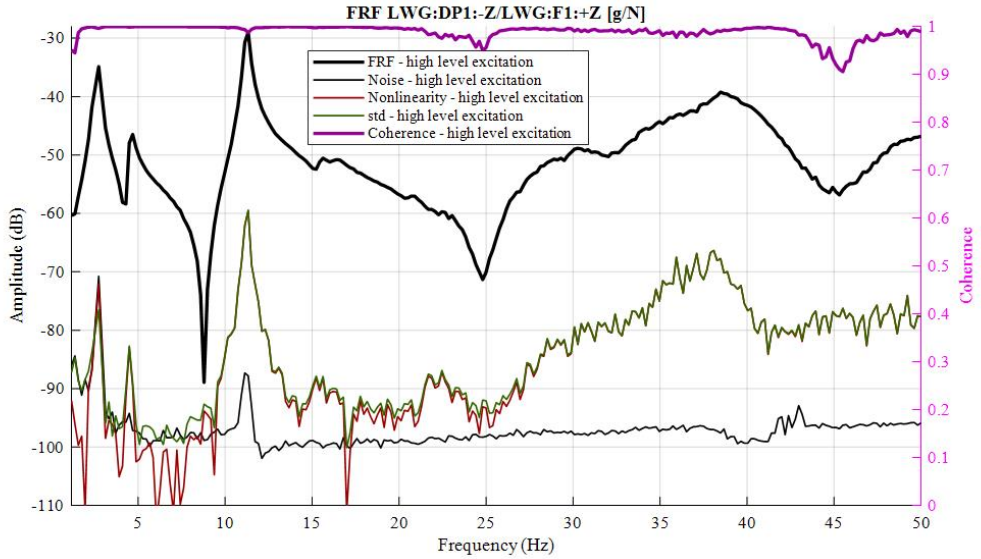

Figure 8: The BLA FRF estimation at high level excitation using the proposed technique taking into account all data.

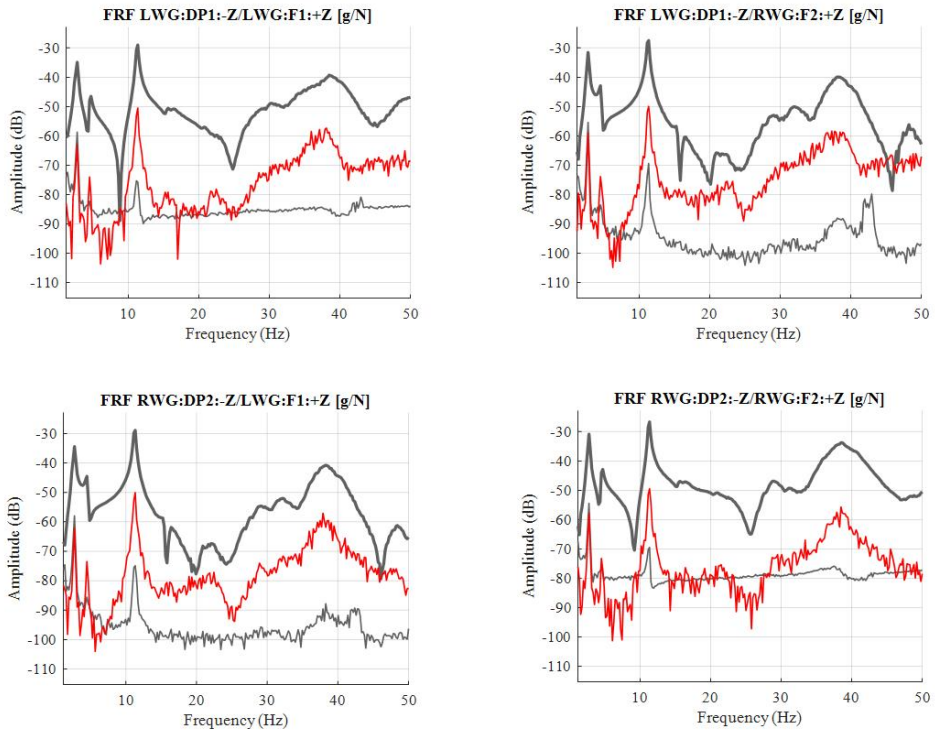

Figure 9: Expected noise and nonlinearity levels at one measurement block (period).

measurement block (period) without using the BLA technique? In this case one has to correct for the number of experiments. This is shown in Figure 9 for both low (lighter colors) and high (darker colors) level excitation. In this case, if the end-user decides to use a simple linear model in his application the error levels would be in order of SNLR. If the end-user decides to opt for an appropriate nonlinear model the error levels would be in order of SNR. The gain (improvement) by the use of an advanced nonlinear model would be approximately the difference between the SNR and SNLR.

3 IN-FLIGHT MEASUREMENTS

After the validation of the FE model with the Ground Vibration Testing activities, the aircraft is allowed to have its first flight and to perform the so-called flutter measurements. Flutter is included in the broader term aeroelasticity, i.e. the study of the static and dynamic response of an elastic airplane. Since flutter involves the problems of interaction between aerodynamics and structural deformation, including inertial effects, at subcritical as well as critical speeds, it really involves all aspects of aeroelasticity [18], [19]. The GVT results are used to perform flutter prediction by using the correlated FE model of the aircraft. Despite all the efforts in developing flutter prediction tools, the only definitive method for clearing aircraft for flutter is flight testing. Aircraft certification procedures require that aircraft manufacturers demonstrate that the flight envelope of a new aircraft is clear from flutter with a high safety margin. Several possibilities exist for exciting the structural modes and performing a flutter test. In the eFusion case, the pilot was asked to impulsively excite the control surfaces and then bringing them back to zero position. Theoretically it is supposed to be a perfect impulse which should be able to excite all the structural modes, but practically it becomes difficult to excite high frequencies. Once the excitation is applied, the aircraft structure's response is measured at several locations. The aircraft was instrumented by means of 12 accelerometers as shown in Figure 10.

Figure 10: Aircraft instrumentation for flutter testing: accelerometers placed on the left wing (left picture), Simcenter SCADAS XS measurement system in the cockpit (middle) and accelerometer on the vertical tail plane (right picture).

The Simcenter SCADAS XS system has been used in-flight to record 12 measurement channels which were placed at the same locations as during the GVT tests. Six flights with different flight points (speed-altitude levels) were measured and the post-processing analysis allowed to identify some of the aircraft modes. Several flights have been performed. The analysis reported in this work focus mainly on the most interesting flight in which stable conditions and clear impacts on the stick could be identified. Figure 11 shows the altitude (red curve), the measured speed (blue curve) and the time history of an accelerometer located on the wingtip and measuring along the vertical direction (green curve). Several time segments are highlighted and they have been further analyzed to estimate the modal parameters in different conditions: takeoff, landing, maximum speed, maximum altitude.

Table 3 lists the modes identified by considering the time segment in which the pilot was ex-

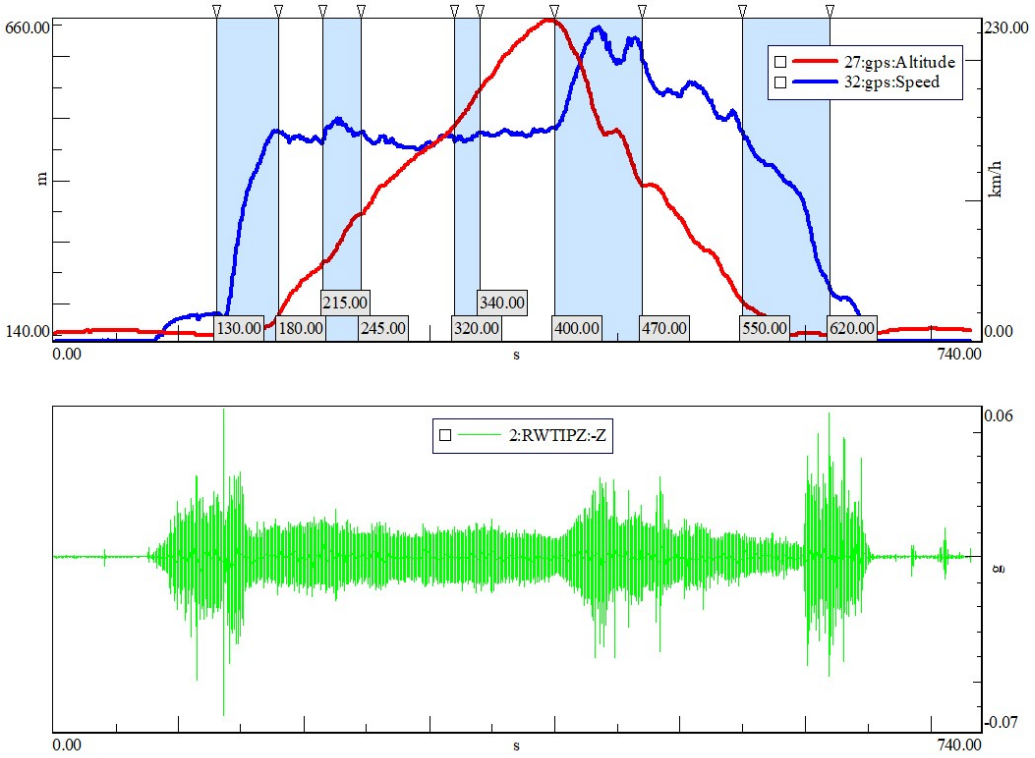

Figure 11: Altitude (red), measured speed (blue) and accelerometer reading (green) along an entire flight.

citing the movable surface by hitting the stick to induce roll and/or pitch of the aircraft at the maximum speed. The natural frequencies and the mode shapes are compared to the GVT modes. Four modes out of the first six mode shapes were well identified with the use of Operational Modal Analysis. More in detail, the Operational Polymax [20] algorithm has been used to estimate the modal parameters from output-only data. The missing two modes could not be identified because of the limited amount of sensors that could be used during the in-flight measurements.

Table 3: eFusion aicraft mode sets (GVT vs in-flight measurements); HTP = Horizontal Tail Plane; VTP = Vertical Tail Plane

Mode n.	**GVT**	**In-flight**	**Δ Frequency**	**Description**
1	10.69	10.59	-0.9%	1^{st} wing bending
2	15.44	15.18	-1.7%	tail torsion
3	16.35	-	-	fuselage bending
4	18.16	-	-	1^{st} HTP bending
5	20.25	20.87	3.1%	1^{st} HTP bending + in-plane wing
6	23.58	25.31	7.3%	1^{st} VTP bending

For visualization purposes, the wing bending mode is plotted in Figure 12 (left picture) in which all measured points are represented by a sphere. On the right for comparison purposes it is reported the same mode measured during the GVT campaign where many points were measured on the ground. The two mode shapes correspond quite well to each other, as also confirmed by a value higher than 0.90 of the Modal Assurance Criterion (MAC).

Figure 13 shows the tracking of natural frequencies along an entire flight. These values have

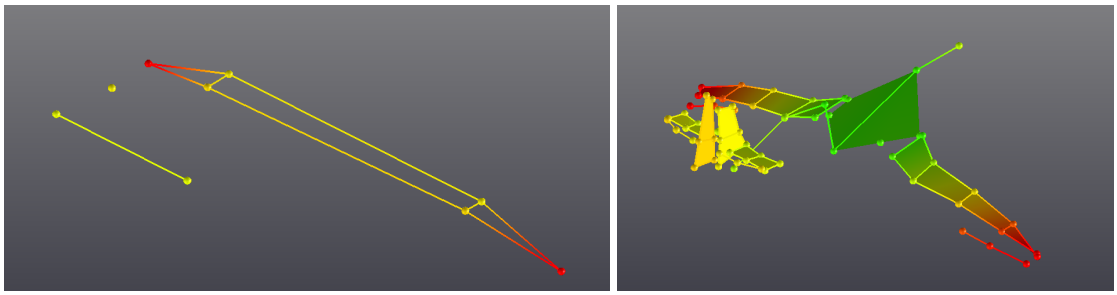

Figure 12: In-flight 1^{st} wing bending (left picture) vs GVT 1^{st} wing bending (right picture).

been obtained by considering 10s time blocks at different conditions. It is quite interesting to see that the natural frequencies do not change significantly along the flight.

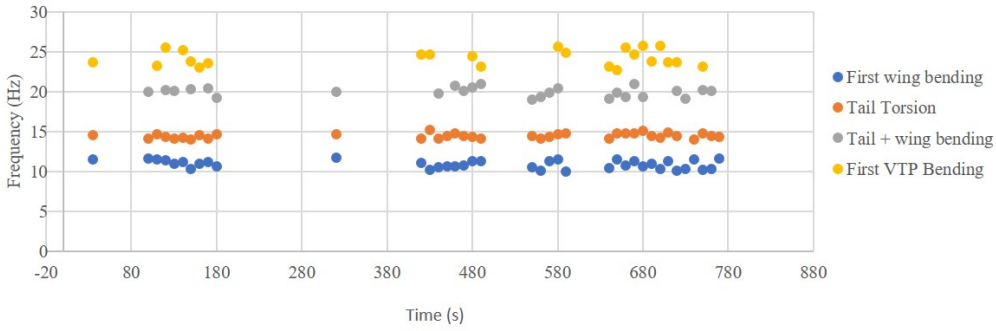

Figure 13: Natural frequencies along an entire flight for the first 4 modes of the aircraft.

Figure 14 shows the damping values obtained for the first two modes with respect to the measured speed. Three different flight conditions are reported here: takeoff, landing and hits zones. Both the first and the second mode have a reasonably constant damping at different speeds (about $2 \pm 0.2\%$ and $1.7 \pm 0.2\%$ respectively).

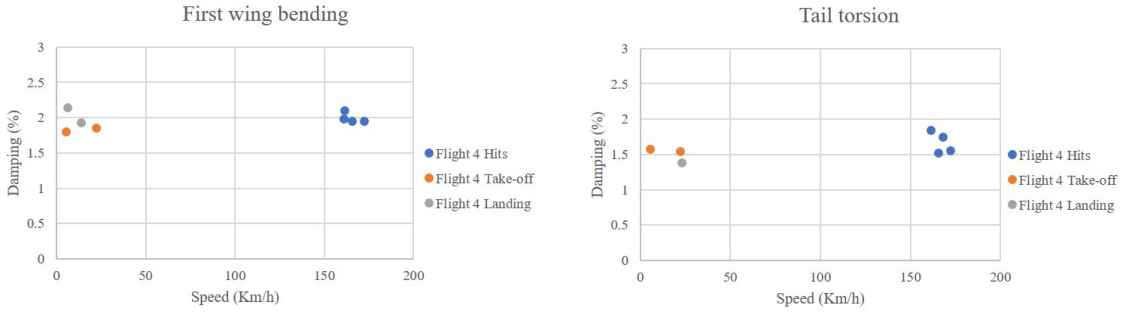

Figure 14: Damping ratios vs speed for the first 2 modes: First wing bending (left) and Tail torsion (right).

4 CONCLUSIONS

This paper aims at characterizing the structural dynamics performance of an all-electric aircaft. The test case has been used to validate the Virtual Driving Point (VDP) technique, an innovative data processing technique which allows a more efficient post-processing and modal parameters identification for Ground Vibration Testing (GVT). The Virtual Driving Point method cancels out the need of performing as many sweeps as shakers in order to compute the system FRFs. Each single sweep is analyzed independently, leading to different modes, whose symmetric or

antisymmetric nature depends on the relative phase between inputs that has been adopted during that run (mainly 0°and 180°). This procedure allows to perform an easier modal analysis, obtaining reliable results in terms of modal parameters. This working principle also leads to advantages related to the system non-linearities and gives, in some cases, the possibility to reduce tests time duration.

In this work a preliminary analysis is presented with the identification of four of the first six modes of the airplane by selecting 10s time blocks from the data measured during several flights. A MIMO Best Linear Approximation framework was also developed to provide a user-friendly interpretation of the nonlinear behavior of MIMO measurement data by extracting user relevant information. The proposed framework turned to be useful for modelling FRFs because:

- orthogonal excitation signals have been provided 1) to improve the SNR, 2) to better characterize the underlying system, 3) to avoid spectral leakage, and 4) to overcome the issues with transient.
- the input and output measurements were characterized,
- the frequency response matrix was estimated and characterized by virtually splitting up the coherence function into noise and nonlinearity level information
- at each amplitude level the noise and nonlinearity information can be retrieved.

Using the provided information potential users can decide if the usage of an advanced nonlinear framework is necessary.

After the validation of the FE model by performing the GVT tests, the electric aircraft was instrumented with a reduced set of sensors to perform some in-flight measurements. An estimate of the stability of each flight condition can be obtained if the damping ratio (related to a certain mode) is plotted against the dynamic pressure. Flutter plots can be drawn by analyzing different flight points acquired during an extensive measurement campaign. The damping ratio trends will be finally plotted for the critical modes in order to determine the flutter conditions which consist in a sudden drop of the damping ratio.

ACKNOWLEDGEMENTS

The authors would like to thank the Siemens eAircraft team as well as the Magnus personnel for their great support during these measurements in Germany and Hungary. This work was funded by the VLAIO Innovation Mandate project number HBC.2016.0235.

5 REFERENCES

[1] UBER Elevate, “Fast-Forwarding to a Future of On-Demand Urban Air Transportation”, Urban Air transportation white paper.

[2] Wall, T., Meyer, R., “A Survey of Hybrid Electric Propulsion for Aircraft”, 53rd AIAA/SAE/ASEE Joint Propulsion Conference, AIAA Propulsion and Energy Forum, (AIAA 2017-4700).

[3] Jansen, R., Bowman, C., Jankovsky, A., Dyson, R., Felder, J., “Overview of NASA Electrified Aircraft Propulsion (EAP) Research for Large Subsonic Transports”, 53rd AIAA/SAE/ASEE Joint Propulsion Conference, AIAA Propulsion and Energy Forum, (AIAA 2017-4701).

[4] Rizzi, S.A., Palumbo, D.L., Rathsam, J., Christian, A.W., Rafaelof, M., "Annoyance to Noise Produced by a Distributed Electric Propulsion High-Lift System", 23rd AIAA/CEAS Aeroacoustics Conference, AIAA AVIATION Forum, (AIAA 2017-4050).

[5] Giclais, S., Lubrina, P., Stephan, C., Boswald, M., Govers, Y., Ufer, J., Botargues, N., "New excitation signals for aircraft ground vibration testing", In Proc. 15th International Forum on Aeroelasticity and Structural Dynamics, IFASD 2011.

[6] Govers, Y., Boswald, M., Lubrina, P., Giclais, S., Stephan, C., Botargues, N., "Airbus a350xwb ground vibration testing: Efficient techniques for customer oriented on-site modal identification", In Proc. Int. Conf. Noise and Vibration Engineering (ISMA 2014).

[7] Napolitano, K., Linehan, D., "Multiple sine sweep excitation for ground vibration tests", In Proc. Int. Modal Analysis Conf. (IMAC XXVII), Orlando, FL, US, 2014.

[8] Hallez, R., Colangeli, C., Cuenca, J., Di Lorenzo, E., Musella, U., Debille, J., "Assessment of the vibro-acoustic performance of an all-electric light aircraft based on ground and in-flight measurements", In Proc. Int. Conf. Noise and Vibration Engineering (ISMA 2018).

[9] Fuellekrug, U., Boeswald, M., Goege, D., Govers, Y., "Measurement of FRFs and modal identification in case of correlated multi-point excitation". Shock Vib 15(3):435-445 (2008).

[10] Peeters, B., Guillaume, P., Van der Auweraer, H., Cauberghe, B., Verboven, P., Leuridan, J., "The PolyMAX frequency-domain method: a new standard for modal parameter estimation?", Shock and Vibration, 11:395-409, 2004.

[11] Schoukens, J., Pintelon, R., Rolain, Y., "Mastering System Identification in 100 exercises", New Jersey: John Wiley & Sons, ISBN:978047093698, 2012.

[12] Dobrowiecki, T., Schoukens, J., "Linear approximation of weakly nonlinear MIMO systems", IEEE International Instrumentation and Measurement Technology Conference (I2MTC), pp. 1607-1612, 2004.

[13] Guillaume, P., Pintelon, R., Schoukens, J., "Accurate estimation of multivariable frequency response functions", 13th World Congress of IFAC, vol.29, no.1, pp.4351-4356, 1996.

[14] Pintelon, R., Schoukens, J., "System Identification: a Frequency Domain Approach", 2nd edition, New Jersey: John Wiley & Sons, ISBN:9780470640371, 2012.

[15] Priemer, R., "Introductory Signal Processing", World Scientific, ISBN:9971509199, 1991.

[16] Csurcsia, P.Z., "Static nonlinearity handling using best linear approximation: An introduction", Pollack Periodica, vol.8, no.1, 2013.

[17] Peeters, B., El Kafafy, M., Guillaume, P., Van der Auweraer, H., "Uncertainty propagation in Experimental Modal Analysis", Conference Proceedings of the Society for Experimental Mechanics Series, 2014.

[18] Cooper, J.E., "Towards faster and safer flight flutter testing", Defense Technical Information Center ADP014182, 2003.

[19] Giclais, S., Lubrina, P., Stephan, "Aircraft Ground Vibration Testing at ONERA", AerospaceLab Journal, ONERA, 2016, p. 1-18.

[20] Peeters, B., Van der Auweraer, H., Vanhollebeke, F., Guillaume, P., "Operational Modal Analysis for estimating the dynamic properties of a stadium during a football game", Shock and Vibration, 14(4):283-03, 2007.

COPYRIGHT STATEMENT